Perovskite Quantum Dots Glasses Based Backlit Displays

Jidong Lin, Yixuan Lu, Xiaoyan Li, Feng Huang,* Changbin Yang, Menglong Liu, Naizhong Jiang, and Daqin Chen*
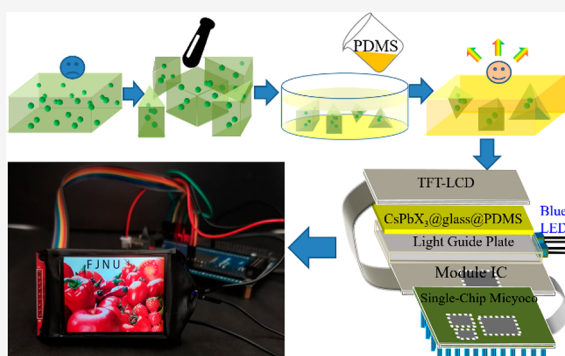
ACCESS | Metrics & More | Article Recommendations | SI Supporting Information

ABSTRACT: Perovskite quantum dots (PeQDs) have been regarded as an alternative to traditional phosphor color converters in the backlit display to improve the color gamut and rendition of LCD. However, the pending barriers of aggregation quenching and structure instability are hindering their practical applications. Herein, high-quality $CsPbX_3$ (X = Br, Br/I) PeQDs were in situ precipitated inside glass to produce nanocomposites with superior optical performance and stability. The highest photoluminescence quantum yield (PLQY) of ~100% for $CsPbBr_3$@glass is ascribed to the elimination of the inner filter effect via a physical dilution approach to restore its apparent value to an intrinsic one, and the exceptional photostability and water/heat resistance are benefited from their effective isolation from the external environment by the surrounding glass network units. Employing the PeQDs@glass@PDMS monolithic film, a high-performance backlit LCD was designed, and its color gamut reached 152% of commercial LCD and 103% of NTSC, demonstrating a great potential in the optoelectronic industry.

The flat-panel display has become one of the most important components in modern optoelectronic products. Currently, requirements for achieving displays with wide color gamut and excellent color rendition are more and more urgent, owing to the dramatically growing demands for a more realistic and low-energy image presentation. Therefore, the development of high-performance white light-emitting diode (wLED) backlights used in the mainstream liquid crystal display (LCD) is needed.[1−4] At present, the commercial backlights in LCDs are mainly composed of InGaN blue chip and Ce: YAG yellow phosphor or blue chip and Eu^{2+}: β-SiAlON green and Mn^{4+}: K_2SiF_6 red phosphor.[5−7] As the human eyes are highly sensitive to the green spectral region, the discovery and development of highly efficient narrowband-emitting phosphors are particularly important to enlarge the color gamut in the display.[8−11] As a consequence, the Ce: YAG yellow phosphor with full-width at half-maximum (fwhm) of ~120 nm and the Eu^{2+}: β-SiAlON green phosphor with fwhm of ~50 nm are not suitable for the future wide-color-gamut display. As an alternative, semiconductor quantum dots (QDs) have been regarded as one of the most compelling candidates for the next-generation backlit display for their intriguing optical properties including high photoluminescence quantum yields (PLQYs), exceptional color purity, and tunable bandgaps.[12−18] Among them, all-inorganic $CsPbX_3$ (X = Cl, Br, I) perovskite QDs (PeQDs)

have recently gained intensive attentions for their facile synthesis, high defect-tolerance, and outstanding optical performance.[19−22]

Unfortunately, perovskite halide materials generally suffer from degradation upon external stimuli (such as moisture, light, and heat) and color segregation of mixtures with different compositions for their inherent ionic crystal feature and low formation energy.[23,24] Great efforts have been recently devoted to address moisture instability and environment sensitivity of perovskite materials. For instance, various strategies including defect passivation, surface encapsulation with dense layers, and embedding in polymer matrices, inorganic salts, zeolite-Y, and silica matrix, among others, have been developed to improve the stability of PeQDs.[25−31] It is worthwhile to mention that inorganic amorphous glass networks can accommodate the $CsPbX_3$ crystalline lattice for their abundant interstitial spaces, and the nanocomposite structure strategy of in situ nucleation/growth of $CsPbX_3$ PeQDs inside the glass matrix (defined as $CsPbX_3$@glass) to enhance passivation of their surface is of
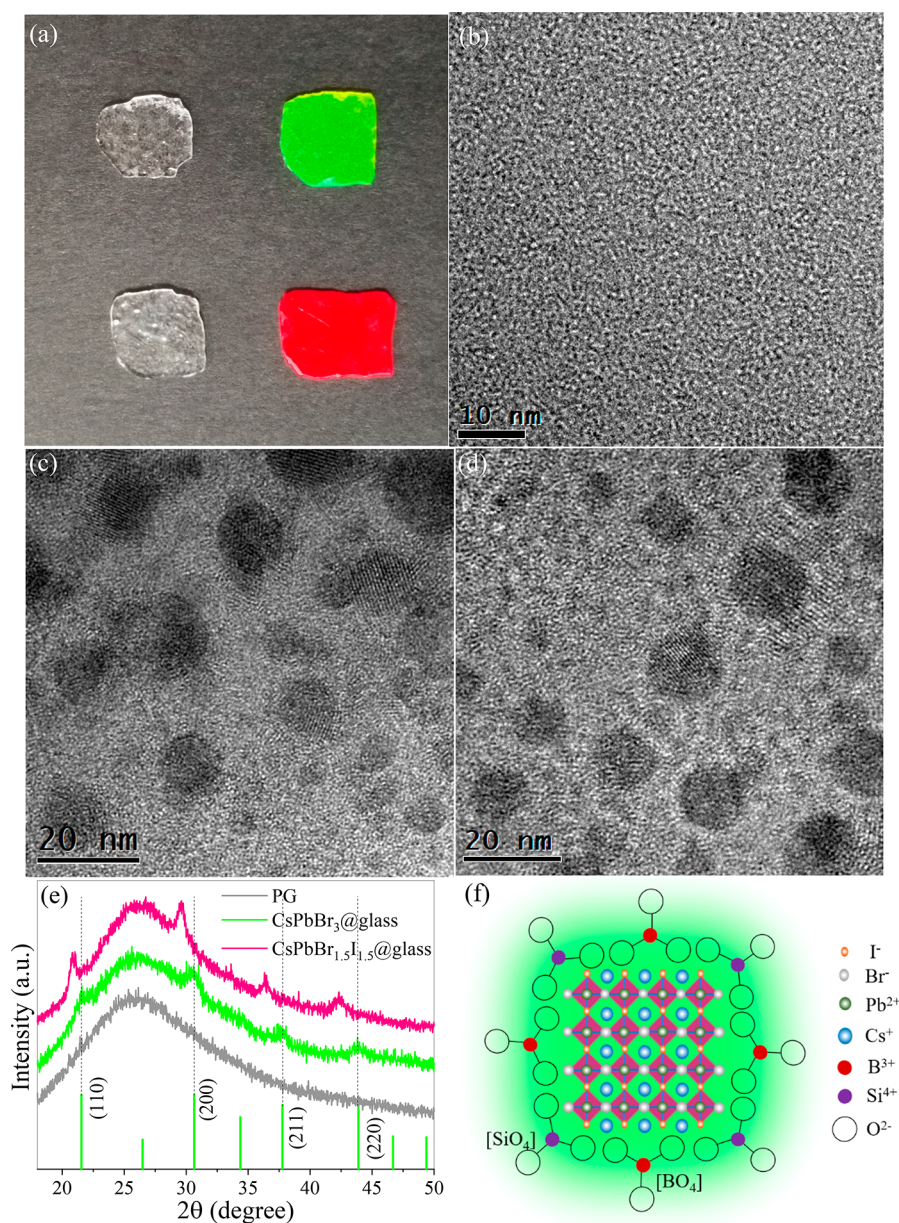
Figure 1. (a) Photographs of precursor glasses and CsPbX$_3$@glass samples (X = Br, Br$_{1.5}$I$_{1.5}$) under daylight. HRTEM images of (b) precursor glass, (c) CsPbBr$_3$@glass, and (d) CsPbBr$_{1.5}$I$_{1.5}$@glass. (e) XRD patterns of precursor glass and the obtained CsPbX$_3$@glass nanocomposites. Bars represent standard diffraction data of cubic CsPbBr$_3$ crystal (JCPDS No. 54-0752). (f) Schematic illustration of CsPbBr$_{1.5}$I$_{1.5}$@glass structure, where the CsPbBr$_{1.5}$I$_{1.5}$ particle resides in the interstices of the glass network and thus is surrounded by the [SiO$_4$], [BO$_4$], and [BO$_3$] structural units.

particular interest.[32−36] An inorganic glass matrix can be regarded as an ideal host for semiconductor QDs benefitting from its compact network configuration and low chemical activity.[37] It can provide a protective insulating layer over the easily degradable CsPbX$_3$, which not only protects the CsPbX$_3$ PeQDs from external environments but also effectively blocks the agglomeration and color segregation among CsPbX$_3$ particles, thereby significantly improving the stability of CsPbX$_3$.[33,38] Unfortunately, most reported PLQYs of CsPbX$_3$@glass composites are still not high enough (Figure S1), which cannot match the colloidal CsPbX$_3$ counterparts, and the genuine factors restraining their PLQYs are pending. Consequently, the corresponding backlit films and devices have not been successfully fabricated, and there is no report concerning their practical applications in backlit displays so far.

Herein, it is demonstrated that the quality of in situ grown PeQDs inside glass is actually high and comparable to colloidal counterparts, and the dominant reason for low PLQYs is ascribed to energy loss by multiple processes of reabsorbing and then re-emitting from the enriched PeQDs in the glass matrix. We provide a simple physical dilution strategy to improve the apparent PLQYs of CsPbX$_3$@glass approaching their intrinsic ones. Indeed, ∼100% PLQY of green CsPbBr$_3$@glass and ∼80% PLQY of red CsPbBr$_{1.5}$I$_{1.5}$@glass composites are achieved, which are believed to be the highest values reported for CsPbX$_3$@glass composites so far (Figure S1). We further embed CsPbX$_3$@glass powders in polydimethylsiloxane (PDMS) to produce homogeneous CsPbX$_3$@glass@PDMS films with near-unity PLQYs and compared their stability with colloidal CsPbX$_3$ PeQDs@PDMS. The as-prepared composite
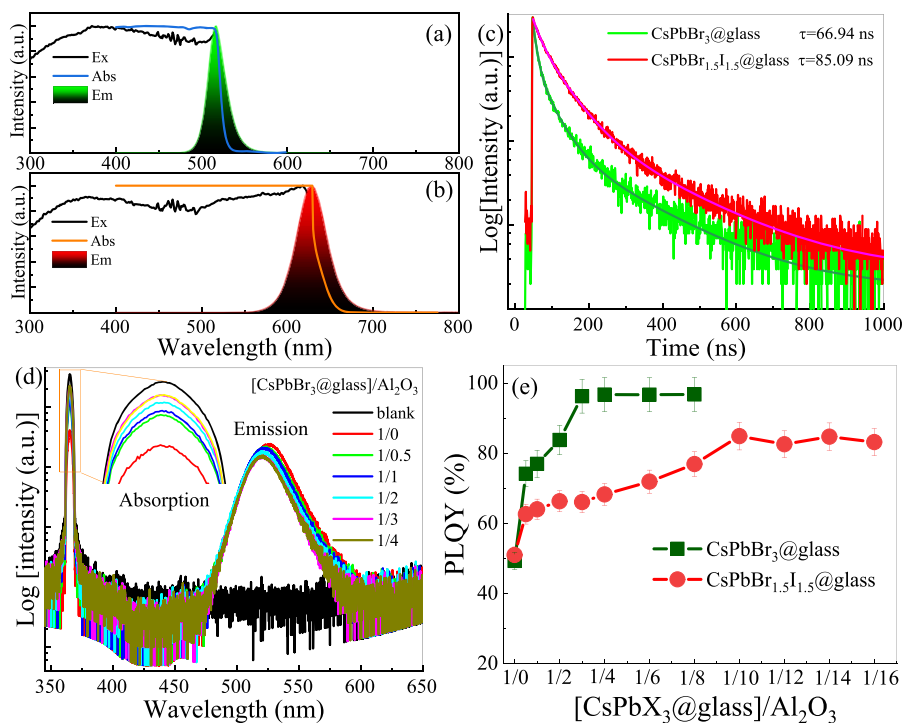
Figure 2. Absorption, excitation, and emission spectra for (a) $CsPbBr_3$@glass and (b) $CsPbBr_{1.5}I_{1.5}$@glass, and (c) the corresponding PL decay curves. (d) Quantitative PL spectra of the $CsPbBr_3$@glass-Al_2O_3 mixture and the reference upon 365 nm excitation to determine PLQYs. (e) Dependence of PLQYs of $CsPbBr_3$@glass on the ratio of $CsPbBr_3$@glass to Al_2O_3.

films exhibit excellent stability against heat/water and UV radiation, where no obvious change in PLQY is found after experiencing UV radiation for 7 days and boiling in water (90 °C) for 24 h. The $CsPbX_3$@glass@PDMS was tested successfully as the backlight in LCD, showing a much wider color gamut. Compared with the screen using a commercial backlight, the demoed $CsPbX_3$@glass LCD intuitively exhibits a more remarkable color rendition and a higher saturation. Besides, the $CsPbX_3$@glass@PDMS films and the designed backlit units present the potential for flexible displays owing to the elastic properties of the PDMS matrix.

The present $CsPbX_3$@glass nanocomposites were prepared by in situ nucleation/growth of the $CsPbX_3$ PeQDs inside the glass matrix, which was achieved by heat-treatment of the specially designed precursor glasses (PGs) with compositions of SiO_2-B_2O_3-ZnO-Cs_2O-PbX_2-NaX (X = Br, I). X-ray photoelectron spectroscopy (XPS) and energy dispersive X-ray (EDX) data confirm the existence of these elements for the as-prepared glasses (Figure S2, Figure S3). As shown in Figure 1a, the precursor glasses are colorless and transparent, and they are converted into bright green and red bulks after glass crystallization, which indicates the successful precipitation of $CsPbX_3$ crystals in the glass network. Notably, benefitting from the facile and cost-effective glass preparation technique, the $CsPbX_3$@glass composites can be easily fabricated on a large scale (Figure S4). Transmission electron microscope (TEM) image verifies the amorphous structure of precursor glass without any contrast (Figure 1b). Typical $CsPbBr_3$ and $CsPbBr_{1.5}I_{1.5}$ crystalline particles with sizes of 10−20 nm are well discerned in the glass matrix (Figure 1c,d and Figure S5). Importantly, high-resolution TEM (HRTEM) observation demonstrates distinctly resolved lattice fringes of $CsPbX_3$ PeQD in glass, confirming its high crystallinity and high quality (inset of Figure S5a). Indeed, an amorphous halo in X-

ray diffraction (XRD) pattern of the precursor glass is observed, and typical cubic $CsPbX_3$ (X = Cl, Br, I) crystalline diffraction peaks are superimposed on the amorphous halo after heat-treatment (Figure 1e). Fourier transform infrared (FTIR) and Raman spectra evidence the existence of Si−O and B−O vibrational structures in the composites (Figure S6, S7). Magic angle spinning nuclear magnetic resonance (MAS NMR) spectra show characteristic resonance bands of $[SiO_4]$, $[BO_3]$, and $[BO_4]$ units (Figure S8). Therefore, it is believed that $CsPbX_3$ PeQDs locate in the interstices of the glass network and they are surrounded by the $[SiO_4]$, $[BO_4]$ and $[BO_3]$ structrual units (Figure 1f and the discussion in Supporting Information), which will be beneficial for them to separate from external environment.

The as-prepared $CsPbX_3$@glass composites exhibit typical narrowband green and red photoluminescence with distinct peaks at 518 and 630 nm (Figure 2a,b), attributing to the band-edge exciton recombination emissions from the embedded $CsPbBr_3$ and $CsPbBr_{1.5}I_{1.5}$ PeQDs, respectively. Both UV−vis absorption and excitation spectra contain strong absorption/excitation edges near 516 and 628 nm correspond to bandgap energies of $CsPbBr_3$ and $CsPbBr_{1.5}I_{1.5}$ (Figure 2a,b). Worthy to be noted, there is only a slight stokes-shift (5−10 meV) between the emission peak and the absorption/excitation edge, which implies the risk of reabsorption for the emitted photons. Time-resolved emission spectra reveal their decays are in nanosecond scale (Figure 2c), further verifying the intrinsic exciton recombination feature of $CsPbX_3$ embedded in glass. The fitted decay lifetime of 67 ns for $CsPbBr_3$@glass and 85 ns for $CsPbBr_{1.5}I_{1.5}$@glass are longer than the values of colloidal PeQDs,[19] which may be attributed to the reduced nonradiative transition and the improved stability of $CsPbX_3$ passivated by the glass network. Taking $CsPbBr_3$@glass as a typical example, temperature-dependence
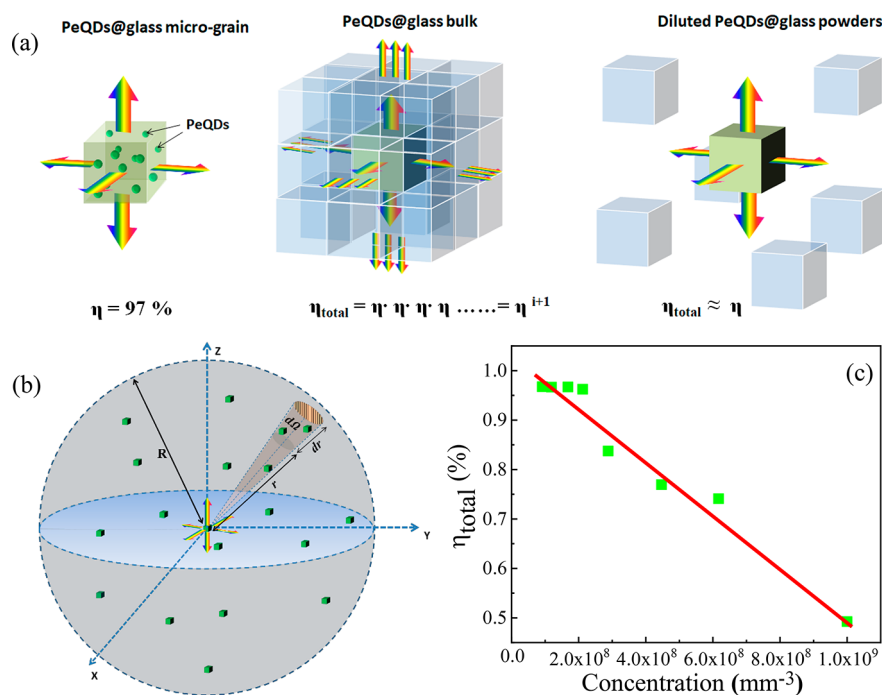
Figure 3. (a) Schematic illustrating the quantum yield diversity between the unabridged CsPbBr$_3$@glass bulk and the diluted glass powders. (b) Spherical coordinate system for simulating the reabsorption and re-emission processes in the CsPbBr$_3$@glass-Al$_2$O$_3$ mixture. (c) The plot of η_{total} versus the concentration of CsPbBr$_3$@glass powders in the CsPbBr$_3$@glass-Al$_2$O$_3$ mixtures. The concentration values are evaluated on the basis of the weight ratio of CsPbBr$_3$@glass to Al$_2$O$_3$ and their densities (Supporting Note S2).

PL spectra were recorded to evaluate exciton binding energy (Figure S9). The obtained value is 107 meV (Figure S9), which is far larger than that (~30−40 meV) of colloidal CsPbBr$_3$ PeQDs.[20] The larger exciton binding energy ensures the survival of excitons at room temperature (26 meV) and even higher temperatures and leads to an improved luminescence efficiency. Quantitative PL spectra for the CsPbBr$_3$@glass sample upon 365 nm UV light excitation were recorded to determine its PLQY of 52% (Figure S10a). Confusingly, such ideal composite configuration, that is, high-quality PeQDs and compact glass matrix passivation, does not lead to desirable PLQYs.

To reveal their intrinsic PLQYs, the CsPbX$_3$@glass composites were ground into fine powders (1−2 μm) and were thoroughly mixed with nonluminescent (inert) Al$_2$O$_3$ powders in different weight ratios. The quantitative PL spectra for the mixtures were recorded (Figure S10b). As evidenced in Figure 2d and Figure S11, with the increase of Al$_2$O$_3$ concentration, the absorption of 365 nm excitation light quickly descends owing to the reduced CsPbBr$_3$ emitting particles in the mixture, while their PL only shows a slight decrease. Additionally, the PL band gradually shifts toward short-wavelength (Figure S12). A similar case is found for the CsPbBr$_{1.5}$I$_{1.5}$@glass sample (Figure S13). As demonstrated in Figure S14, the appearance colors for the mixtures with the reduced CsPbX$_3$@glass content related to Al$_2$O$_3$ gradually fade; however, the intense luminescence is retained. Fluorescence images from the ensemble system and an individual CsPbBr$_3$@glass particle (unit) clearly evidence that each particle can yield green luminescence (Figure S15). Compared with that of the ensemble system, obvious blue-shifting and narrowing of emission from a single CsPbBr$_3$@glass unit are observed (Figure S16). These results indeed verify the existence of frequent reabsorption effect in the

ensemble system, which leads to energy loss (i.e., low PLQY) via multiple reabsorption and re-emission processes. Therefore, the intrinsic PLQY can be obtained by diluting CsPbBr$_3$ concentration with the addition of nonluminescent Al$_2$O$_3$ diluent. Evidently, PLQYs of both CsPbBr$_3$ and CsPbBr$_{1.5}$I$_{1.5}$ gradually enhance with decrease of [CsPbX$_3$@glass]/Al$_2$O$_3$ ratio and reach ~100% and ~80%, respectively (Figure 2e). To the best of our knowledge, these PLQYs represent the highest efficiencies reported for the CsPbX$_3$@glass (X = Br, Br/I) composites (Figure S1). We believe this kind of physical dilution is an effective route to promote PLQYs of CsPbX$_3$ PeQDs and address liability for quenching in both colloidal CsPbX$_3$ powder aggregate and CsPbX$_3$ enriched glass bulk. Notably, different than the case of PLQY, the corresponding external quantum efficiency (EQE) exhibits a gradual decrease from ~50% to ~20% with an increase of inert Al$_2$O$_3$ or PDMS content (Figure S17) because of the reduction of emitting PeQDs content in the composites.

Generally, three factors might affect PLQYs of QDs systems: 1. the quality of QDs;[39] 2. the near-field multipole interactions between neighboring QDs, which is known as Förster resonance energy transfer and occurs within subwavelength range (in a scale of nanometer);[40] 3. the far-field reabsorption among diverse QDs, an effect known as the inner filter effect (IFE), which takes place at a distance larger than emitting wavelength (>1 μm).[41,42] It is experimentally demonstrated, when the CsPbBr$_3$@glass is ground into small sized (1−2 μm, that is, in the far-field scale) powders and diluted by Al$_2$O$_3$ powders, the PLQYs of the mixtures can be significantly raised up to a value close to 100% (Figure 2e). Therefore, it can be concluded that the quality of CsPbBr$_3$ PeQDs inside glass is already as good as colloidal ones, and the near-field energy coupling can also be excluded by considering that millions of PeQDs precipitate in an individual PeQDs@glass unit. Hence,
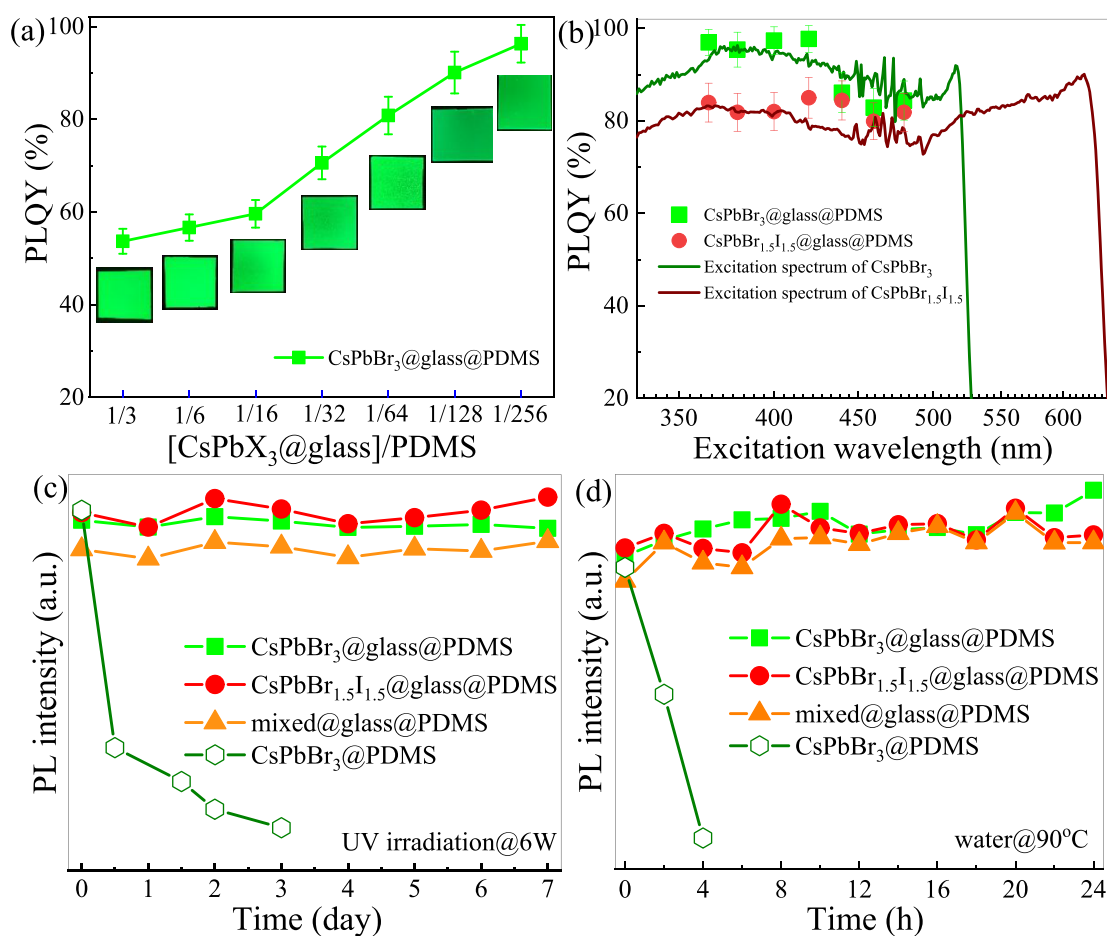
Figure 4. (a) Dependence of PLQYs for the green film (CsPbBr$_3$@glass@PDMS) on the weight ratio of [CsPbBr$_3$@glass]/PDMS. Insets are the photographs of the luminescent films. (b) Dependence of PLQYs for the CsPbBr$_3$@glass@PDMS and CsPbBr$_{1.5}$I$_{1.5}$@glass@PDMS films on the wavelength of incident excitation light. The excitation spectral lines are provided as the guides. (c) Photostability test under UV light (6W) irradiation for 7 days. (d) Humidity-resistance test under the strengthening condition by directly immersing CsPbX$_3$@glass@PDMS films in water maintained at 90 °C for 24 h. As a comparison, the data for colloidal CsPbBr$_3$ PeQDs in PDMS (CsPbBr$_3$@PDMS) are also provided in (c, d).

the far-field reabsorption effect is believed to be the primary factor that restricts PLQY of our CsPbBr$_3$@glass bulk. Figure 3a illustrates a schematic to clarify the far-field reabsorption effect on quantum yield diversity between the bulk and the diluted powders. The PLQY for an individual CsPbBr$_3$@glass unit (1−2 μm) is identified as the intrinsic PLQY (η, ∼100%). For the CsPbBr$_3$@glass bulk or undiluted CsPbBr$_3$@glass powders aggregate, the emitted photons that succeed in yielding from the bulk or the aggregate have experienced multiple reabsorption and re-emission processes, leading to a low PLQY (defined as the apparent PLQY η_{total}, ∼50%).

Mathematically, the apparent PLQY for the glass bulk or the aggregate (η_{total}) is a cumulative product of the intrinsic one (η)

$$\eta_{total} = \prod \eta = \eta^{i+1} \tag{1}$$

where i represents the average time that each photon experiences the reabsorption and re-emission process. Undoubtedly, the value of i can be reduced when the CsPbBr$_3$@glass powders aggregate is diluted by nonluminescent Al$_2$O$_3$ powders. Particularly, when the proportion of the emitting units in the mixture decreases to a threshold value, the value of i would be less than 1 (i.e., approach to zero) and the apparent PLQY η_{total} would approximate to its intrinsic value η.

On the basis of an established spherical coordinate system (Figure 3b), we derive the relationship (Supporting Note S1, S2 and Figures S18, S19) between the value of i and the proportion of PeQDs@glass powders in the mixture (n, the number of PeQDs@glass particles per unit volume)

$$i = 2\pi n A \frac{Rd^2}{8} \tag{2}$$

where A is a constant representing the absorbency of CsPbBr$_3$@glass, R is the macroscale of the mixture (∼1 mm), and d is the mean size of the CsPbBr$_3$@glass particle (∼1 μm). Accordingly, the value of n is 10^9 mm^{-3} for the CsPbBr$_3$@glass bulk or the aggregate. Assuming that intrinsic PLQY of an CsPbBr$_3$@glass unit is ∼97%, the observed apparent PLQY of ∼50% for the bulk or the aggregate corresponds to 20 times of reabsorption and re-emission (i.e., i = 20) based on eq 1. In the case of the PeQDs@glass-Al$_2$O$_3$ mixture, to restore η_{total} up to ∼97%, the value of i must be close to zero. According to eq 2, the calculated value of n should be lowered down to the magnitude of 10^8 mm^{-3}, which agrees well with the experimentally designed n value of 9.2 × 10^7 mm^{-3} for the PeQDs@glass-Al$_2$O$_3$ mixture with a weight ratio of 1:8 (Figure 3c). These estimated results verify that the far-field reabsorption effect is the critical factor to restrain
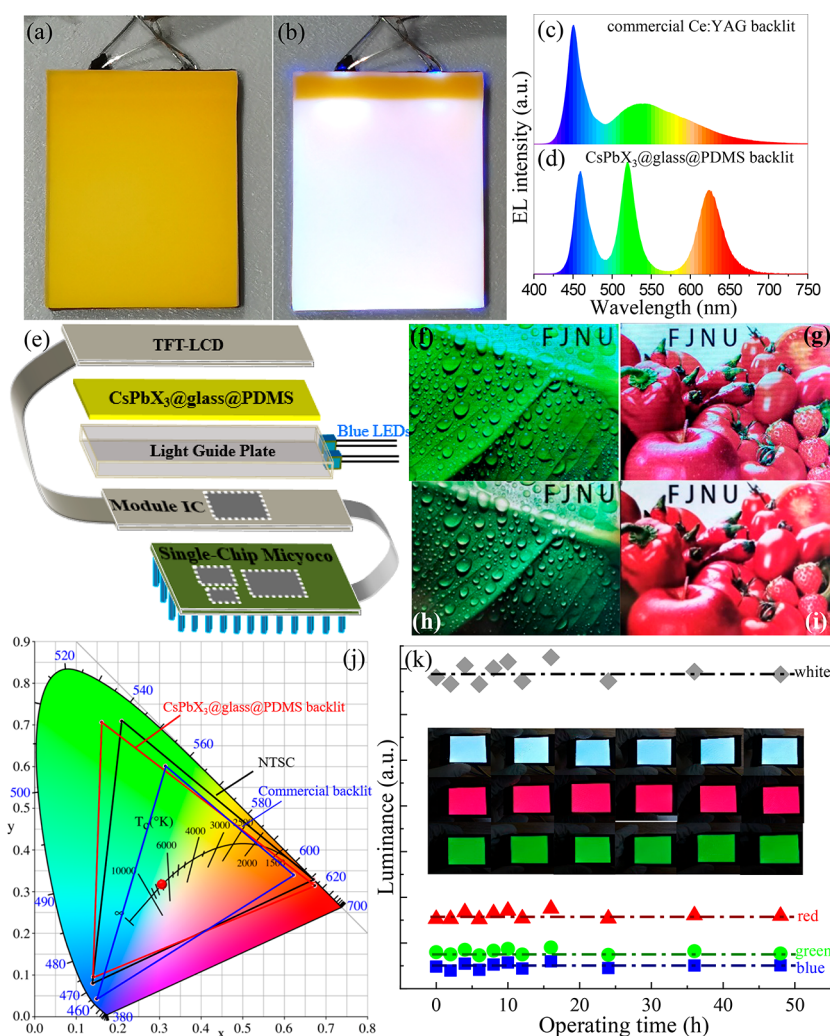
Figure 5. Demonstrations of CsPbX$_3$@glass@PDMS film-based backlight unit with the size of 4 cm × 6 cm: (a) under daylight and (b) under 3.3 V applied voltage. EL spectra of white backlight units using blue LED chips with (c) Ce: YAG yellow phosphor and (d) CsPbX$_3$@glass@ PDMS film. (e) Schematic illustration of LCD device structure using the as-prepared backlight unit. Display performance of LCD screen with (f, g) commercial backlight unit and (h, (i) CsPbX$_3$@glass@PDMS film backlight unit. (j) Color gamut of the commercial screen (blue line), the CsPbX$_3$@glass@PDMS film screen (red line) and NSTC 1953 standard (black line) in the CIE diagram. (k) Variation of luminance of LCD devices with continuous operating times up to 48 h. Insets are the corresponding working green, red, and white LCD devices.

apparent PLQYs of the present CsPbBr$_3$@glass bulk or the CsPbBr$_3$@glass powders aggregate, and the proposed physical dilution strategy is a facile and effective route to restore PLQYs of the composites to their intrinsic ones. Furthermore, with the decrease of the PeQDs@glass content in the composites or films, the corresponding fwhm value exhibits a reduction tendency (Figure S20), further confirming the alleviation of the inner filter effect (i.e., reaborption effect).

Based on the physical dilution strategy, the CsPbX$_3$@glass fine powders were dispersed in PDMS matrix to fabricate the required backlit films to explore their application in LCD (Figure S21). Similarly, adjusting the weight ratio of CsPbX$_3$@ glass to PDMS can modify PLQYs of the films, and increasing the PDMS content related to CsPbBr$_3$@glass will lead to high PLQY up to 95% (Figure 4a). To evaluate whether the CsPbX$_3$@glass@PDMS films are suitable for LCD backlights, excitation-wavelength-dependent PLQYs were determined, as presented in Figure 4b and Figure S22. High PLQYs remain upon 365−480 nm light excitation. Specifically, both green and red CsPbX$_3$@glass@PDMS films show above 80% PLQYs

upon blue light excitation, confirming their suitability as color converters in the blue-chip excited backlight.

In a further experiment, photostability and moisture stability tests for the CsPbX$_3$@glass@PDMS films were carried out. For the photostability test, the composite films were directly irradiated by a UV lamp (6 W) for different durations, and the related PL spectra were recorded. Evidently, no obvious attenuation in PL intensity is observed after UV light irradiation for 7 days (Figure 4c). As a comparison, PL from the colloidal CsPbBr$_3$ PeQDs embedded polymer film (CsPbBr$_3$@PDMS) quickly descends to ∼5% (i.e., ∼90% loss) after UV light irradiation for only 3 days (Figure 4c). For moisture stability, no variation of PLQY is found when exposing the CsPbX$_3$@glass@PMDS film in air for 90 days (Figure S23). Furthermore, the composite films were directly immersed into water and heated at 90 °C for different times. Nearly 100% PL of CsPbX$_3$@glass@PDMS is retained after experiencing the strengthening experiment for 24 h (Figure 4d, Figures S24−S26), while PL of CsPbBr$_3$@PDMS is almost quenched (Figure 4d). All these results certainly verify that the
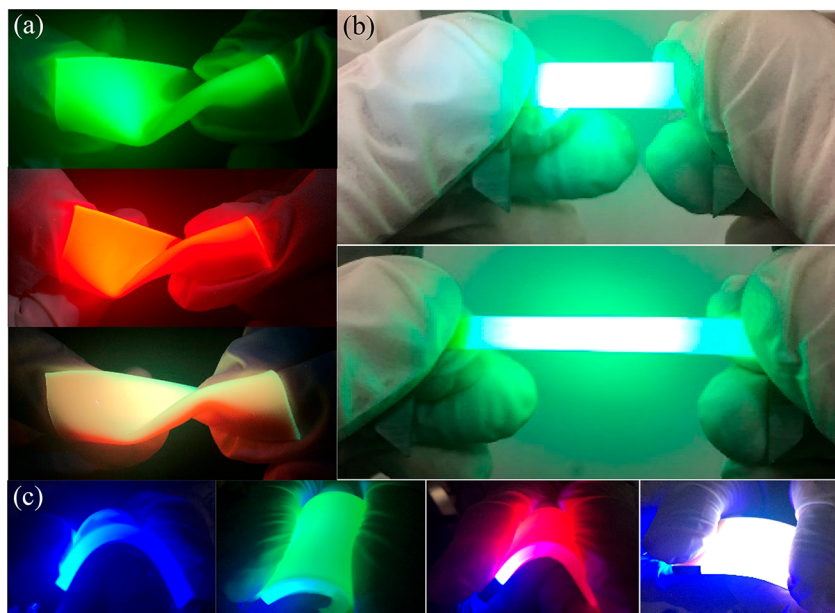
Figure 6. Luminescent photographs of (a) twisted green, red, and yellow CsPbX$_3$@glass@PDMS films. (b) Luminescent photographs of stretched green CsPbBr$_3$@glass@PDMS film. (c) Flexible blue, green, red, and white backlit units upon 3.3 V applied voltage.

present CsPbX$_3$@glass@PDMS films exhibit superior photostability and humidity resistance, which is believed to benefit from the effective protecting role of robust inorganic glass.

With significantly improved PLQYs and stability, the CsPbX$_3$@glass@PDMS yellow film (Figure S21) is potentially applicable in LCD backlights. Notably, in order to avoid detrimental color segregation via halogen anion exchange, the traditional green and red colloidal CsPbX$_3$ films must be separately prepared. Noteworthily, the currently reported color converters generally consist of green PeQDs film and Mn^{4+}: K$_2$SiF$_6$ film stacked above the light guide plate.[15,16,43] Importantly, for the present CsPbX$_3$@glass@PDMS films, dispersing both green CsPbBr$_3$@glass powders and red CsPbBr$_{1.5}$I$_{1.5}$@glass powders in the same PDMS matrix does not induce any change of spectral profiles upon the excitation of a commercial blue chip. As far as we know, this kind of all-PeQDs CsPbX$_3$@glass@PDMS yellow monolithic film (Figure S21) is used in the backlight for the first time. The complete inhibition of halogen anion exchange between CsPbBr$_3$@glass and CsPbBr$_{1.5}$I$_{1.5}$@glass is benefited from the effective passivation of CsPbX$_3$ PeQDs surrounded by [SiO$_4$]/[BO$_x$] glass structural units. We further examine the optoelectronic parameters for the CsPbX$_3$@glass-based LEDs using the on-chip mode (Figure S27). The fabricated LEDs exhibit extremely bright green, red, and white electroluminescence (EL) with maximal luminance and external quantum efficiency (EQE) of 300 000 cd/m^2, 25 000 cd/m^2, 350 000 cd/m^2, and 5.1%, 3.3%, 7.2%, respectively (Figures S28−S30). Such high luminance ensures their practical application in backlit LCD. As shown in Figure 5a,b, the assembly backlight unit yields bright white light at an operating bias of 3.3 V. This voltage is applied on the blue LEDs, which further excite the yellow film to produce the combined white-light luminescence. The corresponding EL spectrum exhibits 450 nm (blue LED chips), 518 nm (green CsPbBr$_3$@glass), and 630 nm (red CsPbBr$_{1.5}$I$_{1.5}$@glass) tricolor narrowband emissions (Figure 5d). As a comparison, the traditional (commercial) backlight is

generally combined by the blue chips and yellow Ce: YAG phosphor with a broadband emission (Figure 5c).

For concept demonstration, a wide color gamut display device (Figure 5e, Figure S31) was successfully designed by using a commercial TFT-LCD panel backlit by the present CsPbX$_3$@glass@PDMS yellow film in combination with blue LED chips in the light guide plate. The inputted images can be modulated and controlled by the single-chip micyoco and the module integrated circuit (IC). The real LCD prototypes intuitively demonstrate the difference of the display performance (Figure 5f−i). Compared with the commercial ones, the LCD screens adopting CsPbX$_3$@glass@PDMS assembly backlight exhibits more details of object colors. For instance, for the display of green color, the commercial screen presents a yellowish green color (Figure 5f), while the assembly backlight unit screen demonstrates a pure green color and a more remarkable color rendition (Figure 5h). Similarly, a pure red color and a high saturation can be realized for the display of red color using the backlight with the CsPbX$_3$@glass@PDMS film (Figure 5i). The color gamut of the as-obtained assembly backlight display was compared with that of commercial backlight display and the standard of NTSC 1953. According to the calculated CIE color coordinates (Table S1), the color gamut of the assembly backlight display is 103% of NTSC 1953 and 152% of that of the commercial backlit display (Figure 5j). To test the stability of the working CsPbX$_3$@glass@PDMS backlight, the EL spectra were recorded after the backlight was lightened for 48 h. As shown in Figure S32 and Figure 5k, blue/green/red tricolor emissions and the yielded white light are stable, and almost 100% EL intensities are remained. Consequently, the (green, red, and white) luminance for the LCD devices remain unchanged after continuously operating for 48 h (insets of Figure 5k).

Finally, we demonstrate that the present CsPbX$_3$@glass@PDMS films are flexible. After these films are severely twisted and stretched, their bright luminescence is maintained without any loss of emitting intensities (Figure 6a,b), confirming a high mechanical endurance owing to the well elastic properties of

PDMS matrix. For instance, the stretching length of CsPbBr$_3$@ glass@PDMS at break can reach as high as ~180% of the original one, while the intense green luminescence is retained (Figure 6b). Furthermore, flexible backlights can be easily achieved by coupling the present films with a homemade bendable light guide plate. As shown in Figure 6c, the bended backlight units yield green, red, and white light by using CsPbBr$_3$@glass@PDMS, CsPbBr$_{1.5}$I$_{1.5}$@glass@PDMS, and mixed@glass@PDMS as color converters, respectively, implying that these CsPbX$_3$@glass@PDMS composite films may find potential applications in flexible displays and other cutting-edge optoelectronic devices.

In conclusion, although metal halide perovskite quantum dots (PeQDs) possess excellent optical properties, their congenital unstable nature is still haunting the prospect of applying in high color rendition backlit display. In situ nucleation/growth of CsPbX$_3$ (X = Cl, Br, I) PeQDs inside inorganic glass has been regarded as a promising approach to produce ultrastable PeQDs@glass composites. Unfortunately, their photoluminescence quantum yields (PLQYs) reported so far are not comparable to those of colloidal counterparts, which remains formidable barriers for their practical applications. In this work, we demonstrated that the low PLQYs for the as-prepared high-quality CsPbX$_3$@glass bulks were primarily attributed to the inner filter effect (i.e., reabsorption effect) from abundant PeQDs in glass medium. A facile physical dilution strategy was proposed to restore their apparent PLQYs to the intrinsic ones via diluting them by nonluminescent (inert) Al$_2$O$_3$ or PDMS polymer, leading to ~100% PLQYs for the CsPbBr$_3$@glass-Al$_2$O$_3$ mixtures and the CsPbBr$_3$@glass@PDMS films. Importantly, the composite films succeeded in passing various harsh stability tests, and no obvious loss in PL was found after experiencing UV radiation for 7 days and boiling in 90 °C water for 24 h. As an application demo, a white LED backlight designed by coupling a yellow composite film with blue chips endowed the LCD with a wide color gamut (152% area of commercial LCD, and 103% of NTSC 1953 standard), confirming a great potential in the optoelectronic industry. Moreover, it is also demonstrated that the CsPbX$_3$@glass@PDMS films and the designed backlit units present the potential for flexible displays because of the well elastic properties of PDMS matrix.

■ ASSOCIATED CONTENT

Ⓢ Supporting Information

The Supporting Information is available free of charge at https://pubs.acs.org/doi/10.1021/acsenergylett.0c02561.

Details of experimental procedures and device fabrication. Additional data pertaining to structrual and spectroscopic characterizations including STEM images, EDX mapping, XPS, FTIR, NMR, Raman spectra, PL spectra, PLQY, EQE and fwhm analyses as well as fluorescence images, and device performance and stability characterizations; deeper discussion on the calculation of the reabsorption processes (PDF)

■ AUTHOR INFORMATION

Corresponding Authors

Feng Huang − College of Physics and Energy, Fujian Normal University, Fuzhou 350117, China; Fujian Provincial Collaborative Innovation Center for Advanced High-Field Superconducting Materials and Engineering, Fuzhou 350117, China; Email: fengh@fjnu.edu.cn

Daqin Chen − College of Physics and Energy, Fujian Normal University, Fuzhou 350117, China; Fujian Science & Technology Innovation Laboratory for Optoelectronic Information of China, Fuzhou 350108, China; Fujian Provincial Engineering Technology Research Center of Solar Energy Conversion and Energy Storage, Fuzhou 350117, China; ⓞ orcid.org/0000-0003-0088-2480; Email: dqchen@fjnu.edu.cn

Authors

Jidong Lin − College of Physics and Energy, Fujian Normal University, Fuzhou 350117, China; Fujian Science & Technology Innovation Laboratory for Optoelectronic Information of China, Fuzhou 350108, China

Yixuan Lu − College of Physics and Energy, Fujian Normal University, Fuzhou 350117, China

Xiaoyan Li − College of Electronics and Information Science, Key Laboratory of Green Perovskites Application of Fujian, Fujian Jiangxia University, Fuzhou 350108, China

Changbin Yang − College of Physics and Energy, Fujian Normal University, Fuzhou 350117, China

Menglong Liu − College of Physics and Energy, Fujian Normal University, Fuzhou 350117, China

Naizhong Jiang − College of Physics and Energy, Fujian Normal University, Fuzhou 350117, China

Complete contact information is available at:
https://pubs.acs.org/10.1021/acsenergylett.0c02561

Notes
The authors declare no competing financial interest.

■ ACKNOWLEDGMENTS

■ REFERENCES

(1) Pust, P.; Schmidt, P. J.; Schnick, W. A. Revolution in Lighting. Nat. Mater. 2015, 14, 454−458.

(2) Zhou, Q.; Bai, Z.; Lu, W. G.; Wang, Y.; Zou, B.; Zhong, H. In Situ Fabrication of Halide Perovskite Nanocrystal-Embedded Polymer Composite Films with Enhanced Photoluminescence for Display Backlights. Adv. Mater. 2016, 28, 9163−9168.

(3) Abe, S.; Joos, J. J.; Martin, L.; Hens, Z.; Smet, P. F. Hybrid Remote Quantum Dots/Powder Phosphor Designs for Display Backlights. Light: Sci. Appl. 2017, 6, e16271.

(4) Zhao, M.; Liao, H.; Ning, L.; Zhang, Q.; Liu, Q.; Xia, Z. Next-Generation Narrow-Band Green-Emitting RbLi(Li$_3$SiO$_4$)$_2$: Eu^{2+} Phosphor for Backlight Display Application. Adv. Mater. 2018, 30, 1802489.

(5) Xia, Z.; Liu, Q. Progress in Discovery and Structural Design of Color Conversion Phosphors for LEDs. Prog. Mater. Sci. 2016, 84, 59−117.

(6) Li, S. X.; Wang, L.; Tang, D. M.; Cho, Y. J.; Liu, X. J.; Zhou, X. T.; Lu, L.; Zhang, L.; Takeda, T.; Hirosaki, N.; Xie, R. J. Achieving High Quantum Efficiency Narrow-Band β-Sialon: Eu^{2+} Phosphors for High-Brightness LCD Backlights by Reducing the Eu^{3+} Luminescence Killer. Chem. Mater. 2018, 30, 494−505.

(7) Zhu, H. M.; Lin, C. C.; Luo, W. Q.; Shu, S.; Liu, Z.; Liu, Y. S.; Kong, J.; Ma, E.; Cao, Y.; Liu, R. S.; Chen, X. Y. Highly Efficient Non-

Rare-Earth Red Emitting Phosphor for Warm White Light-Emitting Diodes. *Nat. Commun.* **2014**, *5*, 4312.

(8) Pust, P.; Weiler, V.; Hecht, C.; Tücks, A.; Wochnik, A. S.; Henβ, A. K.; Wiechert, D.; Scheu, C.; Schmidt, P. J.; Schnick, W. Narrow-Band Red-Emitting Sr[LiAl$_3$N$_4$]: Eu^{2+} as a Next-Generation LED-Phosphor Material. *Nat. Mater.* **2014**, *13*, 891−896.

(9) Takeda, T.; Hirosaki, N.; Funahshi, S.; Xie, R. J. Narrow-Band Green-Emitting Phosphor Ba$_2$LiSi$_7$AlN$_{12}$: Eu^{2+} with High Thermal Stability Discovered by a Single Particle Diagnosis Approach. *Chem. Mater.* **2015**, *27*, 5892−5898.

(10) Zhao, M.; Cao, K.; Liu, M. J.; Zhang, J.; Chen, R.; Zhang, Q. Y.; Xia, Z. G. Dual-Shelled RbLi(Li$_3$SiO$_4$)$_2$: Eu^{2+}@Al$_2$O$_3$@ODTMS Phosphor as Stable Green Emitter for High-Power LED Backlights. *Angew. Chem., Int. Ed.* **2020**, *59*, DOI: 10.1002/anie.202003150

(11) Qin, X.; Liu, X.; Huang, W.; Bettinelli, M.; Liu, X. G. Lanthanide-Activated Phosphors Based on 4f-5d Optical Transitions: Theoretical and Experimental Aspects. *Chem. Rev.* **2017**, *117*, 4488−4527.

(12) Bourzac, K. Quantum Dots Go on Display. *Nature* **2013**, *493*, 283.

(13) Jang, E.; Jun, S.; Jang, H.; Lim, J.; Kim, B.; Kim, Y. White-Light-Emitting Diodes with Quantum Dot Color Converters for Display Backlights. *Adv. Mater.* **2010**, *22*, 3076−3080.

(14) Dai, X. L.; Zhang, Z. X.; Jin, Y. Z.; Niu, Y.; Cao, H. J.; Liang, X. Y.; Chen, L. W.; Wang, J. P.; Peng, X. G. Solution-Processed, High-Performance Light-Emitting Diodes Based on Quantum Dots. *Nature* **2014**, *515*, 96−100.

(15) Zhang, F.; Zhong, H. Z.; Chen, C.; Wu, X. G.; Hu, X. M.; Huang, H. L.; Han, J. B.; Zou, B. S.; Dong, Y. P. Brightly Luminescence and Color-Tunable Colloidal CH$_3$NH$_3$PbX$_3$ (X = Br, I, Cl) Quantum Dots: Potential Alternatives for Display Technology. *ACS Nano* **2015**, *9*, 4533−4542.

(16) Yu, D.; Cao, F.; Gao, Y.; Xiong, Y.; Zeng, H. B. Room-Temperature Ion-Exchange Mediated Self-Assembly toward For-mamidinium Perovskite Nanoplates with Finely Tunable, Ultrapure Green Emissions for Achieving Rec. 2020 displays. *Adv. Funct. Mater.* **2018**, *28*, 1800248.

(17) Won, Y. H.; Cho, O.; Kim, T. Y.; Chung, D. Y.; Kim, T. H.; Chung, H. J.; Jang, H. S.; Lee, J. H.; Kim, D. H.; Jang, E. J. Highly Efficient and Stable InP/ZnSe/ZnS Quantum Dot Light-Emitting Diodes. *Nature* **2019**, *575*, 634−638.

(18) Srivastava, A. K.; Zhang, W.; Schneider, J.; Halpert, J. E.; Rogach, A. L. Luminescent Down-Conversion Semiconductor Quantum Dots and Aligned Quantum Rods for Liquid Crystal Displays. *Adv. Sci.* **2019**, *6*, 1901345.

(19) Protesescu, L.; Yakunin, S.; Bodnarchuk, M. I.; Krieg, F.; Caputo, R.; Hendon, C. H.; Yang, R. X.; Walsh, A.; Kovalenko, M. V. Nanocrystals of Cesium Lad Halide Perovskites (CsPbX$_3$, X = Cl, Br, and I): Novel Optoelectronic Materials Showing Bright Emission with Wide Color Gamut. *Nano Lett.* **2015**, *15*, 3692−3696.

(20) Li, X. M.; Wu, Y.; Zhang, S.; Cai, B.; Gu, Y.; Song, J.; Zeng, H. B. CsPbX$_3$ Quantum Dots for Lighting and Displays: Room-Temperature Synthesis, Photoluminescence Superiorities, Underlying Origins and White Light-Emitting Diodes. *Adv. Funct. Mater.* **2016**, *26*, 2435−2445.

(21) Swarnkar, A.; Chulliyil, R.; Ravi, V. K.; Irfanullah, M.; Chowdhury, A.; Nag, A. Colloidal CsPbBr$_3$ Perovskite Nanocrystals: Luminescence Beyond Traditional Quantum Dots. *Angew. Chem., Int. Ed.* **2015**, *54*, 15424−15428.

(22) Lin, K. B.; Xing, J.; Quan, L. N.; García de Arquer, F. P.; Gong, X. W.; Lu, J. X.; Xie, L. Q.; Zhao, W. J.; Zhang, D.; Yan, C. Z.; Li, W. Q.; Liu, X. Y.; Lu, Y.; Kirman, J.; Sargent, E. H.; Xiong, Q. H.; Wei, Z. H. Perovskite Light-Emitting Diodes with External Quantum Efficiency Exceeding 20%. *Nature* **2018**, *562*, 245−248.

(23) Wei, Y.; Cheng, Z. Y.; Lin, J. An Overview on Enhancing the Stability of Lead Halide Perovskite Quantum Dots and Their Applications in Phosphor-Converted LEDs. *Chem. Soc. Rev.* **2019**, *48*, 310−350.

(24) Wang, X.; Bao, Z.; Chang, Y. C.; Liu, R. S. Perovskite Quantum Dots for Application in High Color Gamut Backlighting Display of Light-Emitting Diodes. *ACS Energy Lett.* **2020**, *5*, 3374−3396.

(25) Wang, H. C.; Lin, S. Y.; Tang, A. C.; Singh, B. P.; Tong, H. C.; Chen, C. Y.; Lee, Y. C.; Tsai, T. L.; Liu, R. S. Mesoporous Silica Particles Integrated with All-Inorganic CsPbBr$_3$ Perovskite Quantum-Dot Nanocomposites (MP-PQDs) with High Stability and Wide Color Gamut Used for Backlight Display. *Angew. Chem.* **2016**, *128*, 8056−8061.

(26) Sun, C.; Zhang, Y.; Ruan, C.; Yin, C. Y.; Wang, X. Y.; Wang, Y. D.; Yu, W. W. Efficient and Stable White LEDs with Silica-Coated Inorganic Perovskite Quantum Dots. *Adv. Mater.* **2016**, *28*, 10088−10094.

(27) Huang, S.; Li, Z.; Kong, L.; Zhu, N.; Shan, A.; Li, L. Enhancing the Stability of CH$_3$NH$_3$PbBr$_3$ Quantum Dots by Embedding in Silica Spheres Derived from TMOS in "Waterless" Toluene. *J. Am. Chem. Soc.* **2016**, *138*, 5749−5752.

(28) Wang, Y. N.; He, J.; Chen, H.; Chen, J. S.; Zhu, R. D.; Ma, P.; Towers, A.; Lin, Y.; Gesquiere, A. J.; Wu, S. T.; Dong, Y. J. Ultrastable, Highly Luminescence Organic-Inorganic Perovskite Polymer Composite Films. *Adv. Mater.* **2016**, *28*, 10710−10717.

(29) Sun, J. Y.; Rabouw, F. T.; Yang, X. F.; Huang, X. Y.; Jing, X. P.; Ye, S.; Zhang, Q. Y. Facile Two-Step Synthesis of All-Inorganic Perovskite CsPbX$_3$ (X = Cl, Br, I) Zeolite-Y Composite Phosphors for Potential Backlight Display Application. *Adv. Funct. Mater.* **2017**, *27*, 1704371.

(30) Loiudice, A.; Saris, S.; Oveisi, E.; Alexander, D. T. L.; Buonsanti, R. CsPbBr$_3$ QD/AlO$_x$ Inorganic Nanocomposites with Exceptional Stability in Water, Light, and Heat. *Angew. Chem., Int. Ed.* **2017**, *56*, 10696−10701.

(31) Krieg, F.; Ochsenbein, S. T.; Yakunin, S.; Brinck, S. T.; Aellen, P.; Süess, A.; Clerc, B.; Guggisberg, D.; Nazarenko, O.; Shynkarenko, Y.; Kumar, S.; Shih, C. J.; Infante, I.; Kovalenko, M. V. Colloidal CsPbX$_3$ (X = Cl, Br, I) Nanocrystals 2.0: Zwitterionic Capping Ligands for Improved Durability and Stability. *ACS Energy Lett.* **2018**, *3*, 641−646.

(32) Ai, B.; Liu, C.; Wang, J.; Xie, J.; Han, J.; Zhao, X. Precipitation and Optical Properties of CsPbBr$_3$ Quantum Dots in Phosphate Glasses. *J. Am. Ceram. Soc.* **2016**, *99*, 2875−2877.

(33) Yuan, S.; Chen, D.; Li, X.; Zhong, J.; Xu, X. In Situ Crystallization Synthesis of CsPbBr$_3$ Perovskite Quantum Dot-Embedded Glasses with Improved Stability for Solid-State Lighting and Random Upconverted Lasing. *ACS Appl. Mater. Interfaces* **2018**, *10*, 18918−18926.

(34) Cheng, Y.; Shen, C.; Shen, L.; Xiang, W.; Liang, X. Tb^{3+}, Eu^{3+} Co-Doped CsPbBr$_3$ QDs Glass with Highly Stable and Luminous Adjustable for White LEDs. *ACS Appl. Mater. Interfaces* **2018**, *10*, 21434−21444.

(35) Ye, Y.; Zhang, W. C.; Zhao, Z. Y.; Wang, J.; Liu, C.; Deng, Z.; Zhao, X. J.; Han, J. J. Highly Luminescent Cesium Lead Halide Perovskite Nanocrystals Stabilized in Glasses for Light-Emitting Applications. *Adv. Opt. Mater.* **2019**, *7*, 1801663.

(36) Yang, C.; Zhuang, B.; Lin, J.; Wang, S.; Liu, M.; Jiang, N.; Chen, D. Q. Ultrastable Glass-Protected All-Inorganic Perovskite Quantum Dots with Finely Tunable Green Emissions for Approaching Rec. 2020 backlit display. *Chem. Eng. J.* **2020**, *398*, 125616.

(37) Xia, M.; Luo, J.; Chen, C.; Liu, H.; Tang, J. Semiconductor Quantum Dots Embedded Inorganic Glasses: Fabrication, Lumines-cent Properties, and Potential Applications. *Adv. Opt. Mater.* **2019**, *7*, 1900851.

(38) Huang, X. J.; Guo, Q. Y.; Yang, D. D.; Xiao, X. D.; Liu, X. F.; Xia, Z. G.; Fan, F. J.; Qiu, J. R.; Dong, G. P. Reversible 3D Laser Printing of Perovskite Quantum Dots Inside a Transparent Medium. *Nat. Photonics* **2020**, *14*, 82−88.

(39) Reiss, P.; Protière, M.; Li, L. Core/Shell Semiconductor Nanocrystals. *Small* **2009**, *5*, 154−168.

(40) Moreels, I.; Justo, Y.; Rainò, G.; Stöferle, T.; Hens, Z.; Mahrt, R. F. Impact of the Band-Edge Fine Structure on the Energy Transfer

between Colloidal Quantum Dots. *Adv. Opt. Mater.* **2014**, *2*, 126−130.

(41) Gan, Z.; Xu, H.; Fu, Y. Photon Reabsorption and Nonradiative Energy Transfer Induced Quenching of Blue Photoluminescence from Aggregated Graphene Quantum Dot. *J. Phys. Chem. C* **2016**, *120*, 29432−29438.

(42) Koc, M. A.; Raja, S. N.; Hanson, L. A.; Nguyen, S. C.; Borys, N. J.; Powers, A. S.; Wu, S.; Takano, K.; Swabeck, J. K.; Olshansky, J. H.; Lin, L. W.; Ritchie, R. O.; Alivisatos, A. P. Characterizing Photon Reabsorption in Quantum Dot-Polymer Composites for Use as Displacement Sensors. *ACS Nano* **2017**, *11*, 2075−2084.

(43) Li, X.; Wen, Z. L.; Ding, S. H.; Fang, F.; Xu, B.; Sun, J. Y.; Liu, C. X.; Wang, K.; Sun, X. W. Facile in Situ Fabrication of Cs_4PbBr_6/$CsPbBr_3$ Nanocomposite Containing Polymer Films for Ultrawide Color Gamut Displays. *Adv. Opt. Mater.* **2020**, *8*, 2000232.